Journal of Hydroscience and Hydraulic Engineering
Vol. 16, No. 1, May, 1998, 117-126

EXPERIMENTAL AND NUMERICAL INVESTIGATION ON ASYMMETRIC OSCILLATORY BOUNDARY LAYERS

By

Hitoshi TANAKA

D. Eng., Professor, Department of Civil Eng. Tohoku University, Aoba-ku, Sendai 980-8579

Ahmad SANA

D. Eng., Formerly Research Associate, ditto

Hiroto YAMAJI

Laboratory Assistant, ditto

and

Mustafa Ataus SAMAD

M. Eng., Research Associate, ditto

SYNOPSIS

A simple piston mechanism has been used to generate asymmetric oscillatory motion in an oscillating tunnel with smooth walls and detailed velocity measurement has been performed by one component LDV under transition from laminar to turbulent flow. The experimental data for mean and fluctuating velocity are presented and comparison has been made with k - ε model prediction. The turbulence generation during deceleration and its distribution in cross-stream direction during acceleration has been found to be qualitatively similar to sinusoidal case. Finally, a friction factor diagram has been proposed for asymmetric oscillatory boundary layers by using predicted model results.

INTRODUCTION

In natural coastal environment, the wave profiles are generally asymmetric due to non-linear effects. A precise estimation of sediment transport under actual field conditions, therefore, requires an adequate knowledge of the properties of asymmetric oscillatory boundary layers. A number of experimental studies have been performed in open flume by various researchers, e.g. Asano et al. (1) and Kuo and Chen (6). But it is difficult to produce a turbulent asymmetric oscillatory boundary layer in an open flume having an adequately thick boundary layer in order to perform detailed measurement. On the other hand, it is possible to generate asymmetric oscillation in an oscillating tunnel, to produce sufficiently high Reynolds numbers and a well defined boundary layer. The asymmetry produced in this case is due to imposed pressure gradient alone, because the continuity condition eliminates the non-linear convection term from the equation of motion. But to impose the

pressure gradient in order to generate an asymmetric oscillation with the help of piston mechanism is also not an easy task. It requires a highly expensive sophisticated equipment to control the piston movement, the reason being for the scarcity of the experiments in this regard. Nadaoka et al. (7, 8) and Ribberink and Al-Salem (10) have performed some experiments by using computer controlled piston systems to study the characteristics of asymmetric oscillatory boundary layers.

Recently, Tanaka et al. (15) proposed a rather simple and inexpensive piston mechanism, by which the asymmetric oscillation is produced mechanically. They performed the experiment under laminar flow to validate this system.

In the present study, this system has been employed to study the properties of asymmetric oscillatory boundary layers on a smooth bottom at higher Reynolds numbers. The numerical prediction for the present cases, which belong to transitional regime between laminar and turbulent flow, has been done by the low Reynolds number k - ε model proposed by Jones and Launder (4). In case of sinusoidal oscillatory boundary layers, this model was found quite efficient (see Justesen (5)). Especially, for the prediction of transitional properties in the sinusoidal boundary layers, this model has been found to be superior to a number of contemporary models of this type, as shown by Sana and Tanaka (12), and Tanaka and Sana (13).

METHODOLOGY

Experimental Conditions

The schematic description of the piston mechanism to generate smooth asymmetric oscillatory motion as proposed by Tanaka et al. (15) along with the oscillating tunnel is shown in Fig. 1. A detailed measurement of velocity was carried out by using one component Laser Doppler Velocimeter (LDV) and the data analysis was performed offline on a PC.

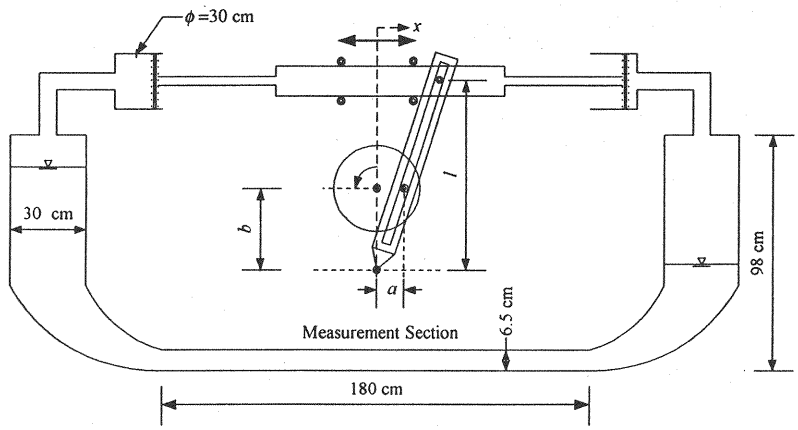

Fig. 1 Schematic description of piston movement system and the oscillating tunnel

Tanaka et al. (15) have shown theoretically that the oscillation generated by the present piston movement system produces an oscillation similar to the one obtained from cnoidal wave theory and by changing the dimensions a, b and l of the system, asymmetry of the wave profile may be changed. Accordingly the non-dimensional velocity of the piston movement was given by

$$u_* = \frac{b_* \cos\omega t - 1}{(b_* - \cos\omega t)^2} \qquad (1)$$

where $u_* = u / \omega l$, u and u_* = dimensional and non-dimensional velocity of piston movement respectively, $b_* = b / a$, ω = angular frequency, and t = time. It was found that with air as working fluid, the temporal velocity variation at the axis of symmetry of the tunnel showed excellent agreement with the cnoidal wave theory. However, due to the restricted length of the tunnel, the use of water as working fluid was inevitable to achieve sufficiently high Reynolds numbers. But in that case, it was necessary to allow the free passage of air into and out of the vertical risers of the tunnel to get the velocity at axis of symmetry in close agreement with the theory, because the performance of the piston movement system under high pressure was not good. Even then perfect agreement with the theory could not be achieved as may be observed from Fig. 2, showing the velocity at axis symmetry for Cases N04, N03 and N02.

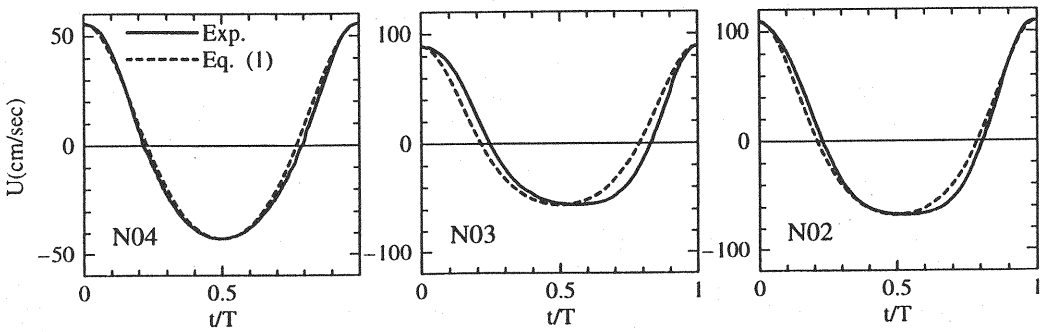

Fig. 2 Velocity at axis of symmetry for Cases N04, N03 and N02

Table 1 shows the experimental conditions for the cases presented herein. In this table, degree of asymmetry $A_s = U_c / (U_c + U_t)$, crest Reynolds number $Re_c = U_c \, \delta_{lc} / \nu$, trough Reynolds number $Re_t = U_t \, \delta_{lt} / \nu$, and U_c and U_t are velocity magnitudes at crest and trough, respectively, where ν being the kinematic viscosity. The Stokes layer thicknesses and time periods for crest and trough are given as δ_{lc} ($=\sqrt{2 \, \nu t_c / \pi}$), δ_{lt} ($=\sqrt{2 \, \nu t_t / \pi}$), t_c and t_t, respectively. The definitions of Re_c and Re_t have been adopted from Nadaoka et al. (6). For numerical computations the values of $RE_c = U_c^2 / \omega\nu$ and $S = U_c / (\omega y_h)$ ($\omega = 2\pi / T$, T = period of oscillation, and y_h = depth to the axis of symmetry) are also provided. All these experiments were carried out for a hydraulically smooth surface.

Table 1. Experimental conditions for asymmetric oscillatory boundary layer

Exp.	T(sec)	t_c(sec)	t_t(sec)	U_c(cm/s)	U_t(cm/s)	A_s	Re_c	Re_t	RE_c	S
N02	2.00	0.84	1.16	109.4	66.9	0.62	859	616	4.38×10^5	10.72
N03	2.38	0.98	1.40	89.3	56.0	0.61	744	559	3.40×10^5	10.41
N04	3.92	1.66	2.26	55.6	42.7	0.57	604	541	2.17×10^5	10.67

k - ε Model

In the present study, the numerical prediction was done by using the original version of low Reynolds number k - ε model by Jones and Launder (4), the governing equations in dimensionless form are expressed by Sana and Tanaka (12). For a particular case, these equations require only

Reynolds number RE_c and Strouhal number S values to provide the solution in dimensionless form.

A Crank-Nicolson type implicit finite difference scheme was employed. In order to achieve a better accuracy near the wall, the grid spacing was allowed to increase exponentially. In space 100 and in time 6000 steps per wave cycle were used. The nonlinear governing equations were solved by iteration method. The convergence limit was set to 5×10^{-5}. The detail in this regard may be found elsewhere (e.g. see Sana and Tanaka (12)).

RESULTS AND DISCUSSIONS

Velocity Profile

For Case N04 it may be noted that the Reynolds number in this case (Re_c = 604, Re_t=541) is at the beginning of transitional range because the value of critical Reynolds number for sinusoidal oscillatory boundary layers is 550, as given by Hino et al. (2). Figure 3 shows the cross-stream velocity profile at selected phases for Case N04. The velocity overshooting at all the phases is stretched in cross-stream direction in comparison with the laminar velocity profiles, which shows the generation of turbulence, though small, causing an increased momentum transport from high velocity regions in cross-stream dimension. The laminar velocity profiles plotted here are as per theory described by Tanaka et al. (14). The velocity profile for Case N04 shows a good agreement with the k - ε model prediction just at the beginning of deceleration phase (t / T = 0.0), especially where the velocity overshooting occurs. But during the course of deceleration, it seems that the model fails to cope with the flow situations. A similar discrepancy was found in case of sinusoidal oscillatory boundary layers also, but in that case, during the deceleration phase, pressure gradient is not so steep as in the present asymmetric case. That is why, in sinusoidal case, the disagreement with the experimental data is not pronounced (see e.g. Sana and Tanaka (12), and Tanaka and Sana (13)).

By using Jensen's definition, according to which the boundary layer thickness, δ, is the distance from the wall to the location of maximum cross-stream velocity at $\omega t = 0$ (or at $\omega t = T/2$), it may be shown that the boundary layer thickness δ is proportional to the Stokes layer thickness ($=\sqrt{\nu T / \pi}$), which suggests that the value of δ must be greater under trough than that under the crest due to longer period of time contained in the trough. The result may be observed at t / T = 0.5 where the boundary layer thickness is greater than that at t / T = 0 from the velocity profiles presented herein. The degree of asymmetry in Case N04 is not so high as may be observed from the value of A_s (=0.57) in this case. That is why the difference between boundary layer thickness under crest and trough is not so significant.

Under increasingly higher Reynolds numbers in Cases N03 and N02, the deviation of the experimental data from laminar velocity profile are more pronounced (Figs. 4 and 5). The diminished velocity overshooting and the stretching in cross-stream direction due to high momentum transport resulting from higher turbulence production became more and more evident here. Gradual increase in near wall velocities between these two cases are also obvious. Although it is not fully developed in Case N03 (Fig. 4) but in Case N02 (Fig. 5) the velocity near the wall so increases that a logarithmic layer is well defined at all phases except near the flow reversal. The model results show gradual deviation, between Cases N03 and N02, from measured velocity profiles in the decelerating phase and thereby, also indicating the inability of the model to predict the velocity profile in deceleration phase. Moreover, it may be observed that the discrepancy between the model prediction and experimental data near the wall during acceleration increases with the increase in the Reynolds number, where the comparison in Case N03 (Fig. 4) is reasonably close, more deviation can be observed in Case N02 (Fig. 5).

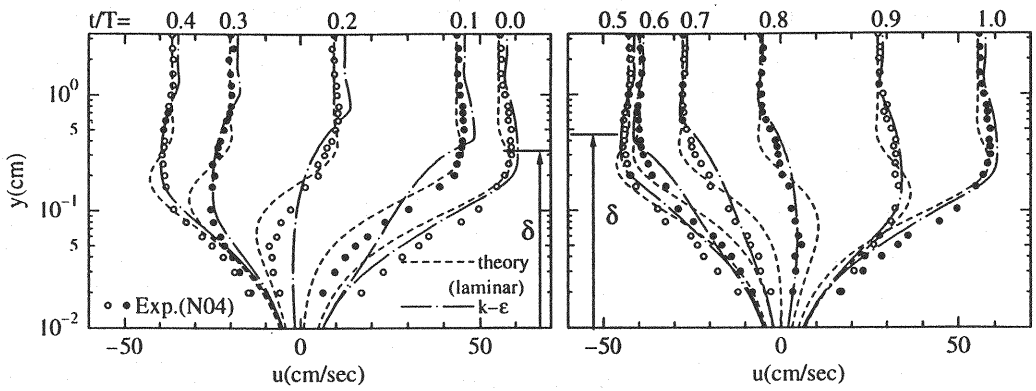

Fig. 3 Velocity profile for Case N04

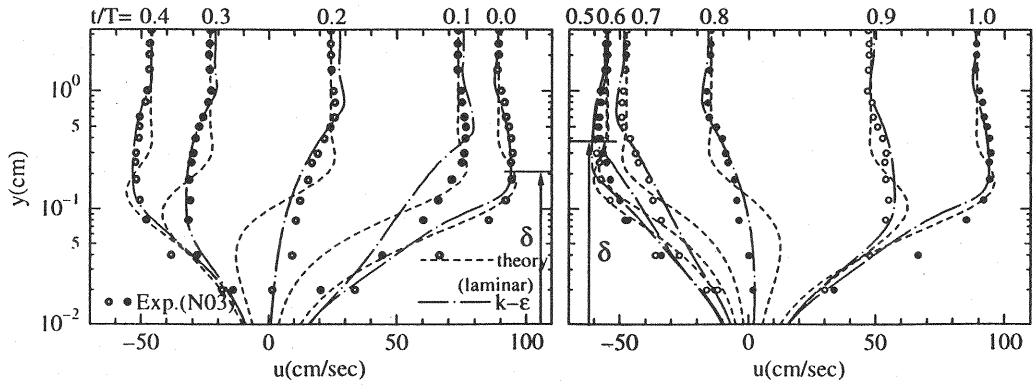

Fig. 4 Velocity profile for Case N03

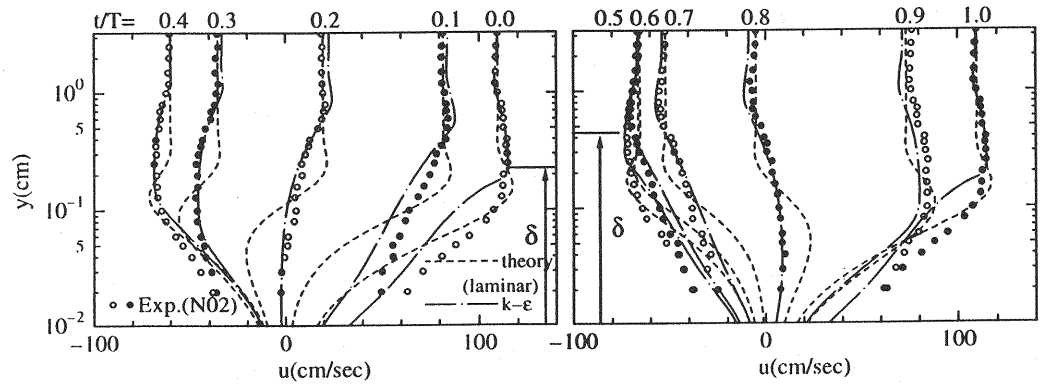

Fig. 5 Velocity profile for Case N02

Since the degree of asymmetry is higher for these cases (A_s=0.61 for Case N03 and A_s=0.62 for Case N02) as compared to Case N04, therefore, the difference of boundary layer thickness under crest and trough is also greater. As indicated before, this difference can be seen to increase with increasing wave asymmetry.

Turbulence Intensity

In a manner similar to that in sinusoidal oscillatory boundary layers, the turbulence is produced in near wall region during deceleration phase as may be observed from Fig. 6 (Case N04) at t / T = 0.0-0.2 and t / T = 0.5-0.7, and it is distributed in cross-stream direction during acceleration phase (t / T = 0.3-0.4, 0.8-0.9). In this case the Reynolds number is close to the critical value as mentioned before, that is why, the turbulence intensity is not so high. Consequently, the cross-stream peak values of u' are located rather far from the wall.

The k - ε model provides the turbulent kinetic energy from which the fluctuating velocity in x direction, u', has been computed using an approximate formula proposed by Nezu (8). The predicted results can then be compared with the experimental data. The equation is given by

$$u' = 1.052\sqrt{k} \tag{2}$$

where k = kinetic turbulent energy. The comparison presented here for u' therefore depends on the degree of accuracy of this approximation as well. For Case N04, the model prediction far from the wall is generally good (Fig. 6). This is also observed for other two cases (see Figs. 7 and 8). For Case N03 (Fig. 7), comparison of predicted fluctuating velocities with measured data, by far, shows considerably good agreement. Although near wall prediction still lags the accuracy for this case, however, at the beginning of decelerating phase (at t / T = 0.0 and 0.5) it can be seen that the turbulence generation is very well simulated. As the Reynolds number gets higher in Case N03 and Case N02, the turbulence intensity can be seen to increase in magnitude but the discrepancy in predicting the shape of near wall fluctuating velocity shows consistent trend for all cases.

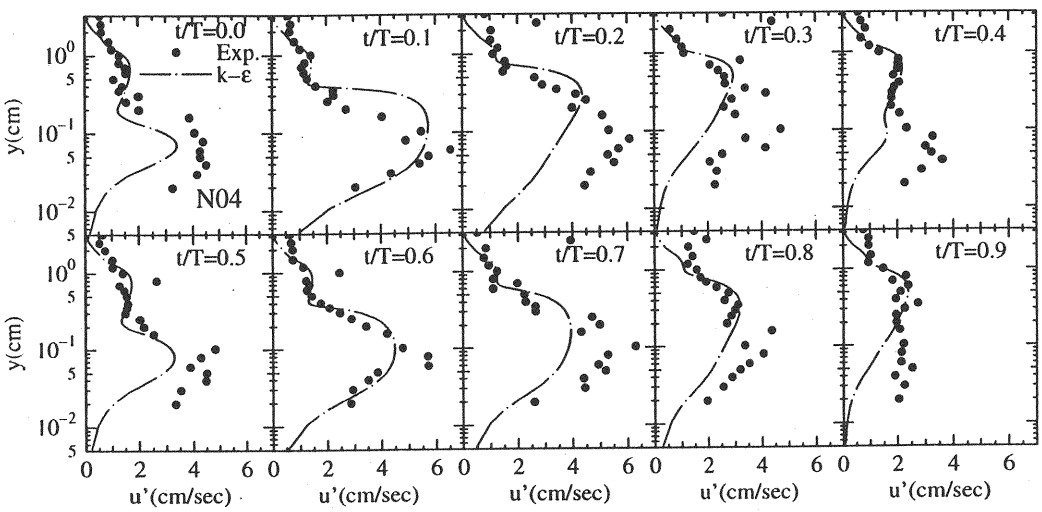

Fig. 6 x-direction fluctuating velocity for Case N04

The peak values of u' for Cases N02 and N03 are located nearer the wall under crest and trough as compared to those at corresponding phases in Case N04. Which suggest higher turbulence production close to the wall at higher Reynolds numbers than in Case N04.

In general it can be noted that although predicted results show significant deviation from measured data, specially at the peaks, at some phases over a range of Reynolds numbers, however, qualitatively it produces very good indication of the pattern of turbulence generation and its mixing.

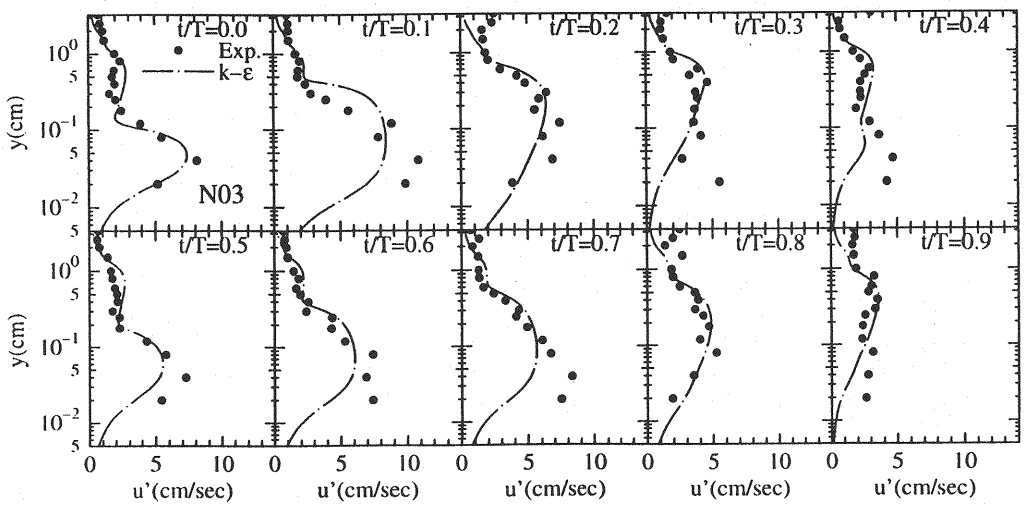

Fig. 7 x-direction fluctuating velocity for Case N03

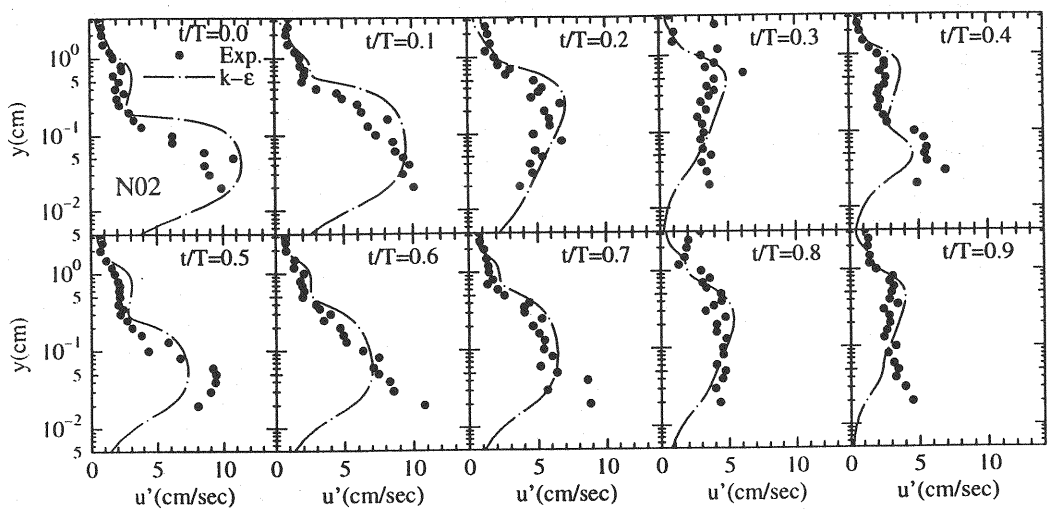

Fig. 8 x-direction fluctuating velocity for Case N02

Friction Factor

In order to compute bottom shear stress from the free-stream velocity, knowledge of the friction factor is important from practical point of view. For sinusoidal oscillatory boundary layers a comprehensive data set is available over a wide range of Reynolds numbers, so that the friction factor diagram may be drawn. On the contrary, for asymmetric oscillatory boundary layers, not only experimental data is scarce, but the studies based on analytical and numerical models are also very few. In the present study, a friction factor diagram has been generated by using the low Reynolds number k - ε model in order to visualize the tentative variation of friction factor with Reynolds number and degree of asymmetry.

It is difficult to define a single friction factor for asymmetric boundary layers, that is why following Tanaka, Sumer and Fredsøe (14), the crest and trough friction factors have been defined separately as:

$$f_{wc}=2.0\tau_{0c}/(\rho U_c^2) \tag{3}$$

and

$$f_{wt}=2.0\tau_{0t}/(\rho U_c^2) \tag{4}$$

where, τ_{0c} and τ_{0t} are maximum values of wall shear stress in crest and trough periods respectively.

This diagram (Fig. 9) shows that for both laminar and turbulent flow, the difference in crest friction factor is not significant for a change in the degree of asymmetry. But in trough phase, A_s value creates a considerable difference in friction factor at a certain Reynolds number. Another interesting feature to note in this figure is that the transition from laminar to turbulent flow requires higher Reynolds number with the increase in A_s value.

The expression for friction factor in case of laminar sinusoidal boundary layer is given by

$$f_w=2/(RE)^{1/2} \tag{5}$$

This has also been plotted in the figure and shows an excellent agreement with asymmetric case at A_s=0.5.

The friction factor for the present experimental data was computed from the wall shear stress profiles obtained by integrating the equation of motion from the wall to axis of symmetry. As may be observed from this figure that the three experiments lie within the transitional region.

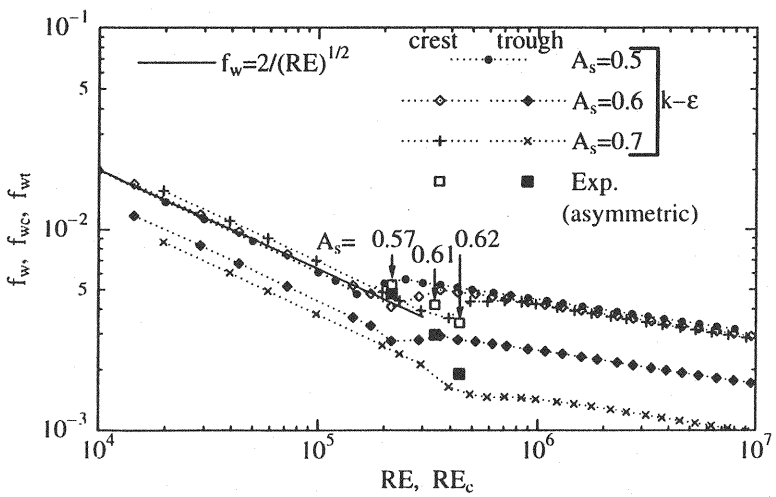

Fig. 9 Friction factor diagram for asymmetric oscillatory boundary layers

The qualitative agreement of the model prediction with the experimental data is satisfactory for all the three cases. Although for Case N04 which corresponds to the beginning of transition, the model underestimates the friction factor at crest and trough, however, the second data set from the

left hand side (N03) shows quite good agreement with the model prediction. For the data set having highest Reynolds number (N02) the model overestimates both the values of f_{wc} and f_{wt}. As may be observed from Fig. 9 that three of the experiments with $A_s \cong 0.6$ depict a gradual transition process similar to that observed in case of sinusoidal oscillatory boundary layers (see e.g. Jensen (3)). On the other hand, the model shows rather abrupt transition from laminar to turbulent flow.

In most of the field situations the flow is turbulent, consequently the part of friction factor diagram relevant to fully turbulent flow is very important. But the experimental data for higher Reynolds numbers are not available as yet, that is why it is difficult to draw the final conclusion regarding the capabilities of the model in fully turbulent regime for asymmetric oscillatory boundary layers.

CONCLUSION

A simple piston movement system has been employed to generate asymmetric oscillatory motion in an oscillating tunnel. The critical Reynolds number for sinusoidal oscillatory boundary layer transition is valid for the asymmetric oscillatory boundary layers with small degree of asymmetry values. The low Reynolds number k - ε model by Jones and Launder (4) showed good performance to predict mean velocity profile during acceleration phase, but during deceleration phase its predictions were not satisfactory. The overall agreement between the model prediction and experimental data is satisfactory for x direction fluctuating velocity. The friction factor diagram produced by the low Reynolds number k - ε model shows that with the change in degree of asymmetry, crest friction factor does not show considerable variation, whereas trough values vary a lot. In order to draw the final conclusion in this regard, the experiments under fully turbulent asymmetric oscillatory boundary layers are required.

ACKNOWLEDGEMENT

The authors gratefully acknowledge the financial support as Grant-in-aid by The Ministry of Education, Science and Culture, Japan for this study.

REFERENCES

1. Asano, T., Amamiya, I. and Iwagaki, Y. : Evaluation of bottom friction factors under finite amplitude waves, Proceedings of the 34th Japanese Conference on Coastal Engineering, pp.1-5, 1987. (in Japanese)
2. Hino, M., Sawamoto, M. and Takasu, S. : Experiments on transition to turbulence in an oscillatory pipe flow, Journal of Fluid Mechanics, Vol.75, pp.193-207, 1976.
3. Jensen, P. : Experimental Investigation of Turbulent Oscillatory Boundary Layers, Series Paper No.45, ISVA, Technical University, Denmark, 1989.
4. Jones, W. P. and Launder, B. E. : The prediction of laminarization with a two equation model of turbulence, International Journal of Heat and Mass Transfer, Vol.15, pp.301-314, 1972.
5. Justesen, P. : Turbulent Wave Boundary Layers, Series Paper No.43, ISVA, Technical University, Denmark, 1988.
6. Kuo, C. T. and Chen, W. J. : Bottom shear stress and friction factor due to the asymmetric wave motion, Proceedings of the 22nd International Conference on Coastal Engineering, pp.637-646, 1990.
7. Nadaoka, N., Yagi, H., Nihei, Y. and Nomoto, K. : Characteristics of turbulence structure in asymmetrical oscillatory flow, Proceedings of the Japanese Conference on Coastal Engineering, Vol.41, pp.141-145, 1994. (in Japanese)
8. Nadaoka, N., Yagi, H., Nihei, Y. and Nomoto, K. : Turbulence structure of asymmetrical

oscillatory flow – dependence on Reynolds number, Proceedings of the Japanese Conference on Coastal Engineering, Vol.43, pp.441-445, 1996. (in Japanese)
9. Nezu, I. : Turbulent structure in open channel flows. Ph.D. Dissertation, Kyoto University, Japan, 1977. (in Japanese)
10. Ribberink, J. S. and Al-Salem, A. : Sheet flow and suspension of sand in oscillatory boundary layers, Coastal Engineering, Vol.25, pp.205-225, 1995.
11. Rodi, W. and Scheuerer, G. : Scrutinizing the k - ε turbulence model under adverse pressure gradient conditions, Transactions, ASME, Journal of the Fluids Engineering, Vol.108, pp.174-179, 1986.
12. Sana, A. and Tanaka, H. : The testing of low Reynolds number k-ε models by DNS data for an oscillatory boundary layer, Flow Modeling and Turbulence Measurements, Vol.6, pp.363-370, 1996.
13. Tanaka, H. and Sana, A. : Numerical study on transition to turbulence in a wave boundary layer, Sediment Transport Mechanisms in Coastal Environments and Rivers, pp.14-25, 1994.
14. Tanaka, H., Sumer, B. M. and Fredsøe : Theoretical and experimental investigation on laminar bounday layer under cnoidal wave motion, Journal of Hydraulics and Coastal Environment Engineering, JSCE, No. 575/II-40, pp.85-90, 1997. (in Japanese)
15. Tanaka, H., Yamaji, H., Sana, A. and Shuto, N. : A new generation method of asymmetric oscillatory flow, Journal of Hydraulics and Coastal Environment Engineering, JSCE, No.565/II-39, pp.111-118, 1997. (in Japanese)

APPENDIX – NOTATION

The following symbols are used in this paper:

A_s = degree of asymmetry;

f_{wc}, f_{wt} = friction factor under wave crest and trough respectively;

k = kinetic turbulent energy;

Re_c, Re_t = crest and trough Reynolds number respectively;

RE_c = wave Reynolds number;

S = Strouhal number;

t_c, t_t = time period of wave crest and trough respectively;

T = wave period;

u' = fluctuating velocity;

U_c, U_t = particle velocity under wave crest and trough;

y_h = depth to the axis of symmetry;

δ_{lc}, δ_{lt} = Stokes layer thickness under wave crest and trough;

ε = turbulent energy dissipation rate;

ρ = water density;

ν = kinematic viscosity of water;

τ_{0c}, τ_{0t} = bottom shear stress under wave crest and trough; and

ω = wave frequency.

(Received November 25, 1997; revised February 17, 1998)